Academic Journal of Applied Sciences
ISSN: 3105-0549 (Print), ISSN: 3105-0557 (Online) | Vol. 2, No. 2, 2026

Passive Shading Optimization for Buildings Based on Differential Evolution and Non-Dominated Sorting Multi-Objective Evolutionary Algorithm

Binhe Wang *, Ran Cheng, Haoran Wu

School of Aeronautics and Astronautics, Sichuan University, Chengdu, China

* **Corresponding author**: (Email: 2891135506@qq.com)

Abstract: This paper proposes an hourly-scale evaluation and multi-objective optimization method for passive shading retrofits in buildings. Using typical meteorological annual data as input, the study couples solar radiation, heat transfer through building envelopes, ventilation heat exchange, window heat gain, and daylighting and glare constraints to construct a computational framework for "design variables—thermal response—energy consumption evaluation." The study employs the Differential Evolution algorithm and the Non-Dominant Sorting Multi-Objective Evolution algorithm to obtain a Pareto optimal solution balancing energy consumption, comfort, and retrofit costs, while incorporating thermal mass coupling and adjustable shading strategies to enhance the model's adaptability. The results indicate that the optimized solution reduces the annual cooling load by 9.4%, heating season energy consumption by 14.7%, and the number of overheating hours by 82.1%. This method is applicable to building shading retrofit decisions across different climate zones and future climate scenarios, demonstrating good universality and engineering application value.

Keywords: Differential Evolution Algorithm, Non-Dominated Sorting Multi-Objective Evolutionary Algorithm, Hourly Weather-Driven Model.

1. Introduction

As energy efficiency requirements for buildings continue to rise, passive technologies have garnered attention due to their low operating costs and high adaptability. External shading can regulate solar heat gain and plays a crucial role in reducing building loads and improving indoor lighting conditions. However, building performance is influenced by a combination of factors—including climate, solar radiation, building envelopes, and operational schedules—and exhibits distinct dynamic characteristics. Traditional methods often rely on typical time points or empirical parameters, making it difficult to reflect annual operational variations or balance the relationship between energy consumption, comfort, and retrofit costs.

Although existing research on building performance optimization has incorporated numerical simulations and intelligent algorithms, many methods still focus on static evaluation or single-objective optimization [1]. They often fail to adequately account for thermal inertia, time-varying meteorological conditions, and cross-climate adaptability, resulting in limitations when implementing these solutions in practice. To address this, this paper constructs an hourly weather-driven framework for building shading evaluation and multi-objective optimization. It establishes mapping relationships among solar radiation, thermal response, and performance metrics, and combines the differential evolution algorithm with multi-objective evolutionary search to obtain Pareto-optimal solutions [2]. Building on this foundation, the study incorporates thermal mass coupling, adjustable shading, and future climate scenarios. Using building passive shading retrofits as a case study, the paper verifies the model's applicability under various climatic conditions, thereby providing a transferable algorithmic framework for building energy-saving retrofits.

2. Passive Shading Optimization Framework Based on Hourly Weather-Driven Model

2.1. Data Description

To evaluate the feasibility of the passive shading retrofit scheme for Academic Hall North, this study uses an hourly weather-driven model to continuously calculate the annual cooling and heating loads. The building is located in a low-latitude, high-radiation environment, where high summer temperatures and classroom glare are relatively serious. Therefore, the main focus of this study is placed on reducing annual cooling energy consumption.

Traditional shading design usually only refers to the solar altitude angle at typical moments such as the summer solstice or winter solstice. However, this static method can hardly reflect the dynamic changes within a day and across seasons. For this reason, TMYx EPW weather data for Haikou are used to construct the boundary conditions for all 8760 hours of the year, including outdoor temperature, direct radiation, diffuse radiation, global horizontal irradiance, and other parameters. These data are then used as dynamic inputs for the subsequent heat balance calculation.

2.2. Hourly Evaluation Model for Passive Shading

Considering the characteristics of low-latitude, high-radiation campus buildings, the shading retrofit is treated as a multi-objective optimization process driven by hourly solar resources. By establishing the mapping relationship among "design variables–heat gain–load response–performance evaluation," different schemes can be compared in a unified way.

The annual hourly sequence is denoted as Tacad , and the occupied period is denoted as Tocc . The outdoor temperature $T_{\text{out}}(t)$, together with the radiation components, determines envelope heat transfer, ventilation heat exchange, and solar radiation input through windows.

The model calculates the solar altitude angle and azimuth angle for each hour, and establishes the solar incidence relationship for the east, west, south, and north façades. Let $\mu_f(t)$ be the cosine of the angle between the solar ray and the façade normal direction. Then the direct radiation on the window surface is expressed as:

$$G_f^{\text{dir}}(t) = I_{DNI}(t)\mu_f(t) \tag{1}$$

Diffuse radiation is approximated as isotropic:

$$G_f(t) = G_f^{\text{dir}}(t) + G_f^{\text{dif}}(t) \tag{2}$$

For the shading configuration, south-facing horizontal overhangs and east–west vertical shading fins are adopted. The design variables $\mathbf{x}$ include overhang depth, fin depth, glass SHGC, and other parameters. The corresponding direct shading coefficient is defined as: $\eta_f^{\text{dir}}(t;\mathbf{x}) \in [0,1]$.

The solar heat gain through the window surface can then be obtained as:

$$Q_f^{\text{sol}}(t;\mathbf{x}) = A_f \cdot SHGC(\mathbf{x}) \cdot \left[\eta_f^{\text{dir}}(t;\mathbf{x})G_f^{\text{dir}}(t) + \eta^{\text{dif}} G_f^{\text{dif}}(t)\right] \tag{3}$$

The total solar heat input of the building is:

$$Q^{\text{sol}}(t;\mathbf{x}) = \sum_f Q_f^{\text{sol}}(t;\mathbf{x}) \tag{4}$$

Based on this, an hourly heat balance model is established:

$$Q^{\text{net}}(t;\mathbf{x}) = Q^{\text{sol}}(t;\mathbf{x}) + Q^{\text{int}}(t) + UA[T_{\text{out}}(t) - T_{\text{set}}] + m(t)c_p[T_{\text{out}}(t) - T_{\text{set}}] \tag{5}$$

Where $Q^{\text{int}}(t)$ is the internal heat gain, while UA and $m(t)$ represent the envelope heat transfer intensity and ventilation heat exchange intensity, respectively.

The hourly cooling and heating demands are defined as:

$$P_{\text{cool}}(t;\mathbf{x}) = \max\left\{0, Q^{\text{net}}(t;\mathbf{x})\right\}, \quad P_{\text{heat}}(t;\mathbf{x}) = \max\left\{0, -Q^{\text{net}}(t;\mathbf{x})\right\} \tag{6}$$

The annual cooling and heating energy consumption are further expressed as:

$$E_{\text{cool}}(\mathbf{x}) = \sum_{t\in\text{Tacad}} P\text{cool}(t;\mathbf{x})\Delta t, \quad E_{\text{heat}}(\mathbf{x}) = \sum_{t\in\text{Tacad}} P\text{heat}(t;\mathbf{x})\Delta t \tag{7}$$

In addition to energy consumption, the model also considers the balance between glare and daylighting. The indoor reference point illuminance $E_{\text{in}}(t;\mathbf{x})$ is used to constrain glare exposure duration and minimum daylighting demand. Stronger shading can reduce cooling loads, but it may also weaken daylight availability. In contrast, relying too much on daylight can easily lead to indoor overheating and glare. Therefore, the whole optimization process is essentially a search for a relatively stable balance among cooling energy consumption, daylighting, and visual comfort.

2.3. Multi-objective Optimization Based on Pareto Frontier

Based on the hourly shading evaluation model, the next step is to identify the trade-offs among different shading schemes. Simply pursuing the lowest cooling energy consumption often results in excessive shading, which may reduce daylight availability, decrease winter solar heat gains, and increase retrofit costs. Therefore, the retrofit process is formulated as a bi-objective optimization problem.

Within the feasible domain Ω, the optimization objective is defined as:

$$\min_{\mathbf{x}\in\Omega}\left(f_1(\mathbf{x}), f_2(\mathbf{x})\right) = \left(E_{\text{cool}}(\mathbf{x}), C(\mathbf{x})\right) \tag{8}$$

Where $E_{\text{cool}}(\mathbf{x})$ represents the annual cooling energy consumption, and $C(\mathbf{x})$ is a cost proxy variable that approximately reflects the retrofit cost associated with shading devices, glazing upgrades, and related measures. The constraints include an upper limit on heating energy consumption, minimum daylighting requirements, and basic comfort criteria, ensuring that the resulting solutions are both energy-efficient and practically usable.

Since the objective functions are evaluated through annual hourly simulations, the mapping from design variables to performance outcomes is a typical black-box problem. The resulting functions generally do not satisfy differentiability or convexity assumptions, making conventional gradient-based methods unsuitable. Differential Evolution (DE) offers better stability for continuous-variable optimization and can accommodate complex constraints, making it suitable for searching the Pareto non-dominated solution set [3].

Each individual in the population generates candidate solutions through differential mutation and crossover operations. The generated solutions are then corrected within the variable bounds to maintain feasibility. Pareto dominance is used to rank and select individuals, and candidate solutions that outperform their predecessors replace the original individuals. This process ultimately produces a set of non-dominated solutions. Compared with a single optimal solution, this approach is more suitable for engineering applications because it provides a range of comparable and selectable design alternatives.

Under the given weather conditions and building parameters, a stable Pareto frontier can be obtained after a limited number of iterations. This provides a unified design-variable basis for the subsequent thermal mass expansion analysis and climate robustness assessment.

Figure 1 shows the final Pareto frontier, illustrating the trade-off between cooling energy consumption and retrofit cost for different shading schemes.

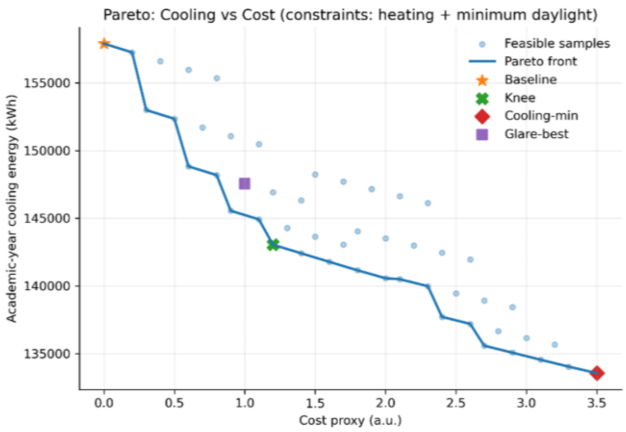

Figure 1. Pareto: Cooling vs Cost

2.4. Retrofit Performance Analysis

Under the heating and minimum daylight constraints, the model generated a total of 50 feasible schemes, including 22 Pareto non-dominated solutions. This indicates that within the current parameter range, no single optimal solution exists, but rather a series of feasible combinations representing different trade-offs.

Figure 1 shows the Pareto frontier between annual cooling energy consumption and retrofit cost. The overall curve exhibits a "steep-front, gentle-back" trend: in the early stage of retrofit, a small cost input can significantly reduce cooling energy consumption; as shading intensity continues to increase, the energy-saving benefit gradually diminishes, and marginal improvement starts to decline.

This phenomenon aligns with the characteristics of buildings in low-latitude, high-radiation regions. For campus buildings like Sungrove University, the cooling load from direct solar radiation accounts for a large proportion, so moderate exterior shading can already significantly reduce window heat gain and alleviate classroom glare. Further increasing shading depth still reduces energy consumption, but the improvement is no longer substantial.

Among the different schemes, the Knee scheme demonstrates better overall performance. Compared with the baseline building, this scheme achieves substantial cooling energy savings under moderate cost conditions while completely eliminating glare periods, making it a key compromise point on the Pareto curve.

In contrast, the Cooling-min scheme further reduces annual cooling energy and peak load, but at a significantly higher cost. Enhanced shading reduces winter solar heat gain, and the decrease in daylight increases lighting energy consumption. Therefore, it is more suitable as an extreme energy-saving boundary rather than a priority solution for practical retrofit.

The Glare-best scheme eliminates glare at relatively low cost, but its cooling energy savings are weaker than Knee, and lighting energy consumption increases more noticeably. This shows that visual comfort and cooling load optimization do not always fully align, and excessive reduction of direct sunlight can sometimes lead to new energy consumption issues.

Overall, the annual simulation results indicate that the Knee scheme achieves a 9.4% reduction in annual cooling energy consumption, while peak cooling load decreases by 3.3%. In addition, glare periods are completely eliminated, and lighting energy consumption increases only slightly. Compared with simply pursuing the lowest energy consumption, this compromise scheme better meets the engineering requirements of actual building retrofits.

3. Dynamic Coupling Model of Shading, Thermal Capacity and Heating

3.1. Coupled Thermal Dynamic Model with Passive Shading

In high-latitude cold regions, fixed shading alone cannot accurately reflect building thermal behavior. For heating-dominated climates such as Borealis, buildings need not only to reduce short-term overheating in summer, but also to make use of winter solar heat gains as much as possible. Therefore, thermal capacity coupling is introduced into the model to describe heat storage and release inside the building.

The shading and glazing parameters are still represented by the design variable $\mathbf{x}$, while the shading state is extended into a schedulable form. The opening and retraction state is represented by $\sigma(t)$. The effective direct shading coefficient is:

$$\eta_{f,\text{eff}}^{\text{dir}}(t;\mathbf{x}) = \sigma(t)\cdot 1 + \big(1-\sigma(t)\big)\eta_f^{\text{dir}}(t;\mathbf{x}) \tag{9}$$

The solar heat gain through the window surface is calculated as:

$$Q_f^{\text{sol}}(t;\mathbf{x}) = A_f SHGC(\mathbf{x})\left[\eta_{f,\text{eff}}^{\text{dir}}(t;\mathbf{x})G_f^{\text{dir}}(t) + \eta^{\text{dif}}G_f^{\text{dif}}(t)\right] \tag{10}$$

The total window solar heat gain is:

$$Q^{\text{sol}}(t;\mathbf{x}) = \sum_f Q_f^{\text{sol}}(t;\mathbf{x}) \tag{11}$$

The indoor building temperature is simplified as a single variable, and the thermal inertia is described by the effective thermal capacity $C_{\text{eff}}(\mathbf{x})$:

$$C_{\text{eff}}(\mathbf{x})\frac{dT}{dt} = H(t;\mathbf{x})[T_{\text{out}}(t) - T(t)] + Q^{\text{sol}}(t;\mathbf{x}) + Q^{\text{int}}(t) + P_{\text{heat}}(t) \tag{12}$$

Where $H(t;\mathbf{x}) = UA(\mathbf{x}) + H_{\text{ve}}(t)$, and $P_{\text{heat}}(t)$ is the heating input.

Under constant parameter conditions, the indoor temperature can be updated through hourly recursion, so that thermal inertia can reflect the actual process of "daytime heat storage–nighttime heat release." During occupied periods, the heating system maintains the minimum comfort temperature and is subject to a power limit to avoid unrealistic unlimited heating.

The annual heating energy consumption is:

$$E_{\text{heat}}(\mathbf{x}) = \sum_{t \in \text{Tacad}} P_{\text{heat}}(t)\Delta t \tag{13}$$

The warm-season overheating index is:

$$OH(\mathbf{x}) = \sum_{t \in \text{Twarm} \cap \text{Tocc}} \max\{0, T(t) - T_{\text{oh}}\Delta t\} \tag{14}$$

At the same time, the accumulated winter solar heat gain $Q^{\text{sol}}(t;\mathbf{x})$ is included in the performance evaluation to measure how well the shading retraction strategy uses passive heat gains.

Overall, this model couples "shading–thermal capacity–heating," allowing the internal thermal inertia of the building to take part in the system response and providing a basis for performance optimization in cold regions.

3.2. Multi-objective Optimization for Borealis Retrofit Design

After thermal-capacity dynamics are introduced, building retrofit in the Borealis scenario is no longer only about reducing heating energy consumption. Shading, heat storage, and indoor comfort are clearly coupled. Strategies that reduce summer overheating may sometimes weaken winter solar heat gains, so the optimization objectives need to consider heating demand, overheating risk, and engineering cost at the same time.

For any design variable $\mathbf{x}$, the model obtains the indoor temperature sequence $T_k(\mathbf{x})$ and the heating power sequence $Q_{\text{heat},k}(\mathbf{x})$ through hourly recursion, and constructs the following multi-objective optimization problem:

$$\min \mathbf{f}(\mathbf{x}) = \left(E_{\text{heat}}(\mathbf{x}), OH(\mathbf{x}), Cost(\mathbf{x})\right) \tag{15}$$

Where $E_{\text{heat}}(\mathbf{x})$ is the total heating-season energy consumption, $OH(\mathbf{x})$ represents the overheating degree-hour indicator, and $Cost(\mathbf{x})$ is used to approximate the engineering cost caused by shading components, glazing upgrades, and thermal capacity configuration.

Since all these indicators come from hourly dynamic simulation, the relationship between design variables and results is still a non-convex black-box mapping. Based on this feature, a non-dominated sorting multi-objective evolutionary algorithm is used for the search to obtain the Pareto trade-off relationships among different objectives [4].

3.3. Thermal Performance Analysis

To verify the applicability of the thermal-capacity-coupled model in cold regions, the baseline building and the optimized scheme are compared based on the Berlin-Tegel typical meteorological year data. The baseline condition uses the "1R1C + heating power limit + warm-up period" setting, where the warm-up period is 168 hours to reduce the influence of initial conditions on the heating statistics.

Under the baseline condition, the total heating-season energy use is 40,247.28 kWh, and the peak heating power reaches 576.00 kW. Figure 2 shows the optimized Pareto frontier. As retrofit cost increases, heating energy consumption keeps decreasing, but the later-stage energy-saving benefit gradually weakens, showing a clear diminishing marginal return.

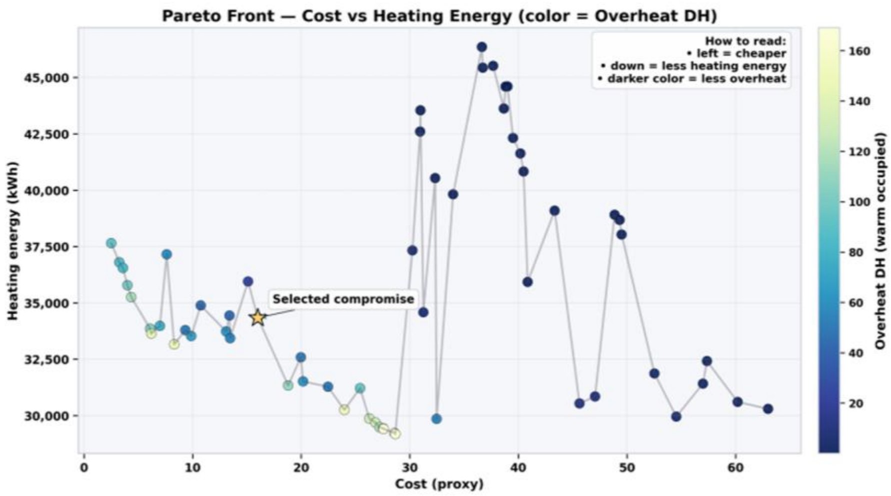

Figure 2. Pareto Front

The baseline scheme corresponds to: $Cost = 0,\quad E_{\text{heat}} = 40{,}247\ \text{kWh}.$

The final selected compromise scheme is located in the medium-cost region: $Cost \approx 15.996$.

At this point, the heating-season energy use decreases to: $E_{\text{heat}} = 34{,}339\ \text{kWh}$.

At the same time, the overheating indicator decreases to: $OH = 31.91$.

The results show that after introducing thermal capacity and schedulable shading, the building can effectively reduce short-term summer overheating risk while maintaining winter heating performance.

Table 1 gives a detailed comparison between the baseline building and the final scheme.

Table 1. Performance comparison between baseline and selected design

Metric	Baseline	Selected	Change	Constraint / Threshold
Heating-season heating energy use	40,247.28	34,339.32	-14.7%	-
Overheating degree-hours (DH)	178.72	31.91	-82.1%	≤ 169.78
Overheating hours	245	85	-65.3%	≤ 232
Underheating degree-hours (DH)	102.31	70.66	-30.9%	≤ 97.19
Underheating hours	70	64	-8.6%	≤ 66
95th-percentile heating power (P95)	23.06	17.65	-23.5%	-
Peak heating power	576.0	576.0	0	cap = 576
Winter solar heat gains	48,596.66	57,349.81	+18.0%	-
Winter gain ratio (winter_ratio)	1.0	1.180	+18.0%	≥ 0.85
Cost proxy	0	15.996	+15.996	-

From the results, the optimized scheme improves several indicators. The total heating-season energy use decreases by 14.7%, the warm-season overheating degree-hours are reduced by more than 80%, and the P95 heating power decreases from 23.06 kW to 17.65 kW. This indicates that the thermal capacity effect smooths indoor load fluctuations to some extent.

In addition, winter solar heat gains increase by 18.0%, suggesting that the shading retraction strategy can improve the use of passive heat gains in cold regions. Overall, this scheme does not simply pursue the lowest energy use. Instead, it forms a relatively stable balance among heating demand, overheating control, and indoor comfort, which better matches the needs of practical engineering retrofits.

4. Model Transferability Analysis Based on Cross-Climate Scenarios

4.1. Adaptable Hourly Evaluation Across Locations

To examine the applicability of the model under different climate conditions, the hourly evaluation model is extended to multiple locations. EPW typical meteorological year data are used for each region, including hourly outdoor temperature and solar radiation. Geographic coordinates are also used to calculate solar altitude and azimuth angles. The building geometry and window-to-wall ratio remain unchanged, so the differences across locations mainly come from climate boundary conditions and changes in solar incidence.

In the cross-site comparison, the daylight aggregation coefficient η_{day} is calibrated at the baseline site and then fixed for the other regions, so that the results remain comparable. For any location ℓ, the retrofit scheme is still optimized within the feasible domain $\Omega^{(\ell)}$ as a bi-objective problem [5]:

$$\min_{\mathbf{x}\in\Omega^{(\ell)}} \left(f_1^{(\ell)}(\mathbf{x}), f_2(\mathbf{x})\right) = \left(E_{\text{cool}}^{(\ell)}(\mathbf{x}), C(\mathbf{x})\right) \quad (16)$$

Where $C(\mathbf{x})$ represents the retrofit cost of shading components, glazing upgrades, and related measures. The constraints include minimum daylighting requirements, glare limits, and the condition that heating energy consumption should not become clearly worse.

4.2. Numerical Validation and Cross-Location Results

To verify the stability of the model, two typical climate types are selected for comparison: one is a cooling-dominated low-latitude region, and the other is a heating-dominated high-latitude region.

Figure 3 compares the results for Berlin and Milano. Overall, at the low-cost investment stage, heating energy consumption decreases relatively clearly. As the investment continues to increase, the energy-saving benefit gradually weakens, showing a typical diminishing marginal return.

Under the same conditions, Milano shows a much larger energy-saving potential than Berlin. This suggests that mild climates can benefit more easily from passive strategies, while cold regions have a stronger “irreducible” heating baseline due to higher envelope heat loss.

After the overheating constraint is introduced, the Pareto frontier for Berlin becomes more strongly restricted. Stronger shading can reduce summer overheating, but it also increases winter heating demand. Therefore, feasible schemes are more concentrated near the constraint boundary.

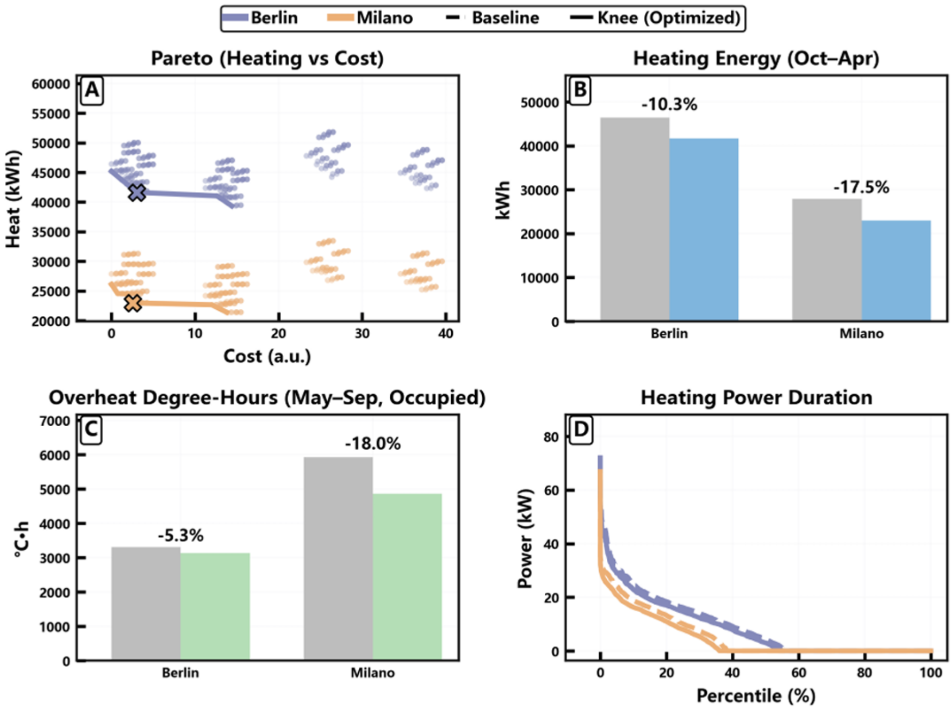

Figure 3. Berlin vs Milano

Overall, the cross-site results show that the benefit direction and magnitude of the same passive strategy are not consistent across different climates. Effective shading design is not simply about increasing obstruction. It needs to balance energy savings, heating demand, and comfort according to local load characteristics.

5. Passive Shading Optimization Strategy Driven by Future Climate Pathways

5.1. Hourly Evaluation Driven by Future Climate Pathways

Under future climate conditions, building retrofits need not only to reduce current energy consumption, but also to cope with long-term warming trends and high-temperature heatwave events. For the four façades of the Student Center, the effect of passive shading and envelope parameter combinations on annual energy use, peak load, and glare performance is analyzed.

The study uses multiple future climate pathways, constructing hourly outdoor temperature sequences through linear interpolation:

$$\Delta T_p(y) = \mathrm{Interp}y_j, \Delta T_{p,y_j} \tag{17}$$

$$T_{\mathrm{out},p,y}(t) = T_{\mathrm{out},0}(t) + \Delta T_p(y) + \Delta T_{p,y}^{HW}(t) \tag{18}$$

Where $\Delta T_{p,y}^{HW}(t)$ represents additional temperature increase under heatwave conditions. If the scenario provides a radiation scaling factor s_p, solar radiation is adjusted accordingly:

$$DNI_{p,y}(t) = s_p DNI_0(t), \quad DHI_{p,y}(t) = s_p DHI_0(t), \quad GHI_{p,y}(t) = s_p GHI_0(t) \tag{19}$$

Then, combining solar altitude and azimuth angles, the hourly irradiance on each façade is calculated for subsequent heat gain and daylighting analysis.

5.2. Solar Shading Parameterization and Hourly Coupling

The Student Center mainly adopts south-facing horizontal overhangs and east–west vertical fins. The design variables are defined as: $\mathbf{x} = (D, F, SHGC, ACH)$.

Where $S_{b,k}(t;\mathbf{x})$ represents the direct shading coefficient on each window, and the diffuse portion uses a fixed transmittance S_d. The solar heat gain through windows is expressed as:

$$Q_{\mathrm{solar}}(t;\mathbf{x}) = \sum_k A_{w,k} SHGC\left[S_{b,k}(t;\mathbf{x}) I_{\mathrm{dir},k}(t) + S_d I_{\mathrm{dif},k}(t)\right] \tag{20}$$

The indoor reference-point illuminance is expressed as:

$$E_{\mathrm{in}}(t;\mathbf{x}) = \eta_{\mathrm{day}} E_{\mathrm{ext}}(t;\mathbf{x}) \tag{21}$$

The glare hours during occupied periods are defined as:

$$H_{\mathrm{glare}}(\mathbf{x}) = \sum_{t\in\Omega_{\mathrm{occ}}} 1_{E_{\mathrm{in}}(t;\mathbf{x})>E_{\mathrm{glare}}} \tag{22}$$

Meanwhile, the lighting load is counted in both indoor heat gain and total energy consumption:

$$E_{\mathrm{light},p,y}(\mathbf{x}) = \sum_{t\in\Omega_{\mathrm{occ}}} P_{\mathrm{light}}(t;\mathbf{x})\Delta t \tag{23}$$

$$Q_{\mathrm{int}}(t;\mathbf{x}) = Q_{\mathrm{base}}(t) + P_{\mathrm{light}}(t;\mathbf{x}) \tag{24}$$

In this way, the model realizes dynamic coupling among "shading—daylighting—energy use" [6].

5.3. Cost-Energy-Peak Trade-off Formulation

Based on the hourly evaluation model, the optimization problem forms a trade-off among cost, energy use, and peak load within the feasible engineering range. The design variable $\mathbf{x}$ is constrained by upper and lower bounds, while daylighting and glare limits are included in the construction of the objective function, so that each climate scenario $(p, y^{\mathring{a}})$ corresponds to a computable objective $J_p(\mathbf{x})$.

The whole evaluation process completes solar radiation calculation, shading correction, window heat gain estimation, thermal state recursion, and energy-use and glare statistics in sequence. In this way, passive shading optimization under future climate conditions can be carried out. Since this process is based on hourly numerical simulation, it does not rely on differentiability or analytical-solution assumptions, and the optimization algorithm can search directly over the full calculation chain.

5.4. Climate-Robust Performance Analysis

To reflect the uncertainty of future climate, the IPCC RCP/SSP framework is used to construct different climate pathways, which are then used as external drivers for annual and decadal load simulations.

Figure 4 shows the changes in cooling energy consumption and peak load over the coming decades under different SSP pathways. Under the baseline condition, all pathways increase over time and gradually diverge in later periods, with higher-forcing scenarios corresponding to higher annual cooling demand. In comparison, peak load increases more slowly, but the overall trend remains consistent.

After optimization, annual cooling energy consumption and peak load decrease clearly under all pathways, indicating that the scheme has good adaptability under different future climate conditions. It is worth noting that the optimal design variables obtained under the five SSP pathways remain the same, suggesting that the optimization result has strong robustness under the current constraints.

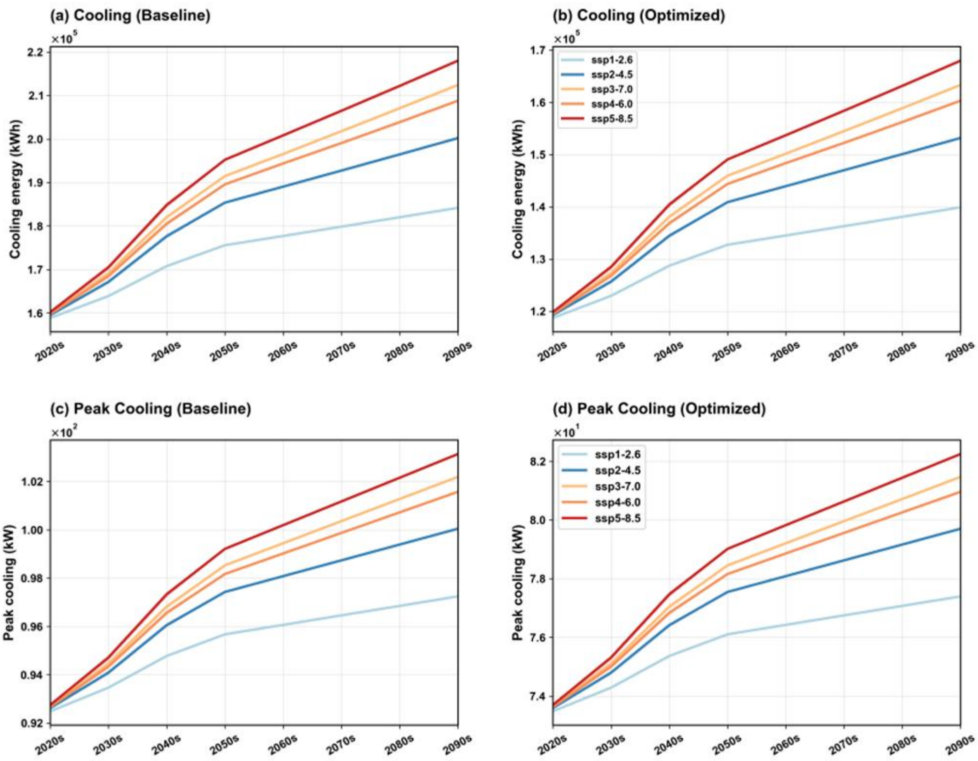

Figure 4. Cooling and peak cooling

6. Conclusions

This paper develops an hourly weather-driven optimization model for passive solar shading in buildings, enabling a coordinated analysis of solar radiation, thermal response, daylighting performance, and retrofit costs. The study demonstrates that the model can identify the trade-off between energy consumption and comfort and generate alternative optimization solutions. In low-latitude, high-radiation regions, the optimized solution reduces the annual cooling load by 9.4% and eliminates glare; in heating-dominated regions, energy consumption during the heating season is reduced by 14.7%, and the number of overheating hours is reduced by 82.1%. Validation across different climate zones and future climate scenarios demonstrates that the model possesses good adaptability and robustness, providing decision support for building energy-saving retrofits. Future research could further integrate real-time operational data and intelligent control strategies to enhance the model's engineering application value.

References

[1] Song, Y., Huang, J. E., Ding, F. H., et al. (2025). Multi-objective optimization of thermal performance of building envelopes based on the uniform design method. Science, Technology and Engineering, 25(35), 15195-15205.

[2] Hou, Y., Wu, Y. L., Bai, X., et al. (2023). A multi-objective differential evolution algorithm with data-driven selection strategies. Control and Decision, 38(7), 1816-1824. https://doi.org/10.13195/j.kzyjc.2021.1957

[3] Yan, L., Ma, J. H., Chai, X. C., et al. (2023). Knowledge-guided adaptive dynamic multimodal differential evolution algorithm. Control and Decision, 38(11), 3048-3056. https://doi.org/10.13195/j.kzyjc.2022.0168

[4] Zheng, Q. (2006). Research and application of a non-dominance sorting genetic algorithm with elite strategy [Master's thesis]. Zhejiang University.

[5] Cao, X. Y., Yu, W., Xiong, J., et al. (2022). Energy-saving technical solutions for residential buildings in regions with hot summers and cold winters based on energy consumption limits. HVAC, 52(7), 41-52. https://doi.org/10.19991/j.hvac1971.2022.07.05

[6] Wang, Y. Y., Wang, T. Y. (2023). Multi-objective optimization of solar curtain walls for office buildings based on photoclimatic zones. Journal of Lighting Engineering, 34(6), 75-81. https://doi.org/10.3969/j.issn.1004-440X.2023.06.008